THE JOURNAL OF PHYSICAL CHEMISTRY B

Article

pubs.acs.org/JPCB

Adsorption of β-Casein–Surfactant Mixed Layers at the Air–Water Interface Evaluated by Interfacial Rheology

Armando Maestro,[†,⊥] Csaba Kotsmar,[‡,§] Aliyar Javadi,[§] Reinhard Miller,[§] Francisco Ortega,[†] and Ramón G. Rubio*[,†]

[†]Departamento de Química Física I, Universidad Complutense de Madrid, Ciudad Universitaria s/n, 28040-Madrid, Spain

[‡]Department of Chemical and Biomolecular Engineering, University of California at Berkeley, Berkeley, California, United States

[§]Max-Planck Institute of Colloids and Interfaces, Potsdam-Golm, Germany

ABSTRACT: This work presents a detailed study of the dilational viscoelastic moduli of the adsorption layers of the milk protein β-casein (BCS) and a surfactant at the liquid/air interface, over a broad frequency range. Two complementary techniques have been used: a drop profile tensiometry technique and an excited capillary wave method, ECW. Two different surfactants were studied: the nonionic dodecyldimethylphosphine oxide (C_{12}DMPO) and the cationic dodecyltrimethylammonium bromide (DoTAB). The interfacial dilational elasticity and viscosity are very sensitive to the composition of protein–surfactant mixed adsorption layers at the air/water interface. Two different dynamic processes have been observed for the two systems studied, whose characteristic frequencies are close to 0.01 and 100 Hz. In both systems, the surface elasticity was found to show a maximum when plotted versus the surfactant concentration. However, at frequencies above 50 Hz the surface elasticity of BCS + C_{12}DMPO is higher than the one of the aqueous BCS solution over most of the surfactant concentration range, whereas for the BCS + DoTAB it is smaller for high surfactant concentrations and higher at low concentrations. The BCS–surfactant interaction modifies the BCS random coil structure via electrostatic and/or hydrophobic interactions, leading to a competitive adsorption of the BCS–surfactant complexes with the free, unbound surfactant molecules. Increasing the surfactant concentration decreases the adsorbed proteins. However, the BCS molecules are rather strongly bound to the interface due to their large adsorption energy. The results have been fitted to the model proposed by C. Kotsmar et al. (*J. Phys. Chem. B* **2009**, *113*, 103). Even though the model describes well the concentration dependence of the limiting elasticity, it does not properly describe its frequency dependence.

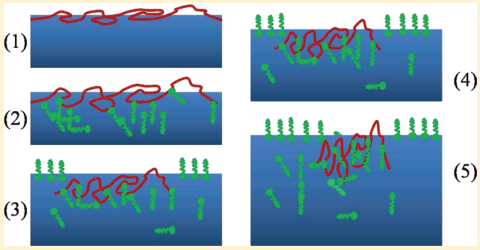

1. INTRODUCTION

It is well-known that the interaction between proteins and surfactant molecules in aqueous solutions leads to interfacial complexes that modify the properties of liquid–fluid interfaces not only by decreasing the surface tension upon adsorption but also by changing their viscoelastic properties.[1−3] This makes the protein–surfactant complexes very important in the formation and stabilization of foams and emulsions in many technological processes in food processing and in the cosmetic and pharmaceutical industry.[2] The physical interactions stabilizing these complexes can be of hydrophobic and/or electrostatic nature[4,5] and can modify the conformation of the protein molecules with respect to that in the bulk.[6] Moreover, it is well-known that after adsorption at a liquid/fluid interface some proteins denature even in the absence of surfactants.[3,7] In addition, the surfactant concentration strongly affects the complexation process and the complex characteristics; e.g., in the case of ionic surfactants, even a net charge inversion can take place.[8] As a consequence, the adsorption layer composition and the properties of the protein–surfactant mixtures at the interface can be highly concentration dependent. Usually, increasing the surfactant concentration, the free surfactant molecules can gradually displace the protein molecules from the surface layer due to a competitive adsorption mechanism. For surfactant concentrations high enough, protein molecules can be completely displaced by surfactants depending on the nature of the protein, the surfactant, the pH and the ionic strength.[9]

Even though the adsorption dynamics of protein–surfactant complexes has been experimentally studied, the exact mechanism for protein displacement is not yet completely understood.[9] Different mechanisms have been suggested based on the competitive adsorption combined with protein modification via complexation.[9] In an attempt to shed light on this problem, we have focused our research on the interfacial viscoelastic behavior of a protein, bovine milk β-casein (BCS). It is a random coil protein with only 1–10% of the chain in a α-helix and less than 25% in a β-sheet structure; indeed it is the most hydrophobic protein of the casein family. At pH = 7 the net charge of the protein is −15 *e*, *e* being the absolute value of the electron charge, indeed, from its primary structure it is possible to demonstrate that about 20 negative charges are

Received: February 1, 2012
Revised: March 23, 2012
Published: April 4, 2012

concentrated in the 50 amino acid residues of the N-terminal portion, and that it represents 1/3 of the total charge at pH = 7. Also, the rest of the chain is relatively hydrophobic, specially the last 40 residues at the C-terminal end, thus making BCS strongly surface active. Contrary to the ordered three-dimensional structures frequently found in proteins, BCS is disordered and flexible, and thus it behaves as a polyelectrolyte with a strong tendency for self-assembling.[10,11] Due to its technological importance, many studies have been published on the BCS adsorption dynamics, mostly using the Langmuir trough and pendant drop methods,[12−14] and several adsorption kinetic models and equations of state have been proposed to describe its interfacial behavior. Moreover, the interfacial rheology of aqueous BCS solutions has also attracted attention in the past few years.[9,10] Graham and Phillips suggested that the frequency dependence of the dilational modulus of BCS is due to the loop/train relaxation at the interface, while other globular proteins, e.g., β-lactoglobulin, are rigid and their dilational modulus was frequency independent. Dickinson, van Vliet et al., and Radke and co-workers have carried out interfacial rheology experiments for BCS films,[15−17] and it was suggested that these protein films form interfacial layers that behave as gel-like networks.[15,16]

Thermodynamic and kinetic models have been developed to describe the adsorption of proteins and protein−surfactant mixtures at liquid interfaces quantitatively. Multiple adsorption states of protein molecules at the surface and an intrinsic compressibility of the surface layer formed have been assumed.[18] Figure 1 shows a scheme of the suggested

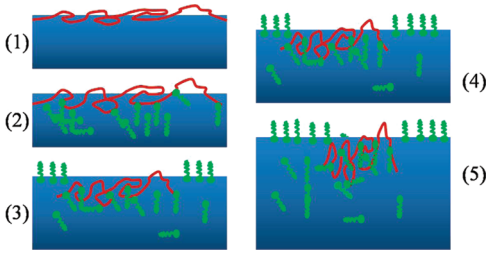

Figure 1. Possible conformational changes of a BCS molecule (red line) at the air/water interface as the surfactant (green objects) concentration increases: (1) very low concentration, (5) high surfactant concentration.

competitive adsorption mechanism between BCS and surfactant molecules at the liquid/air surface at increasing surfactant concentration. Theoretical models for describing the dilational rheological behavior of protein−surfactant and surfactant−surfactant mixtures have been developed recently.[9,19] Indeed, the theory of Lucassen−van den Tempel[20] for interfacial layers of single surfactants has been generalized for the adsorption kinetics of mixtures of an arbitrary number of surface-active species.[19]

As already mentioned, almost all the experimental studies have focused on the low-frequency dynamics (below 1 Hz) of the protein layers,[21] while it is well-known that in many industrial processes, e.g., emulsion production in food technology, the interfaces are subject to fast mechanical deformations that correspond to much higher frequencies. Therefore, in order to have a full understanding of the role of interfacial rheology on the stabilization of emulsions, studies at high frequencies are necessary.

In the present work, we have carried out an experimental and theoretical study of the interfacial rheological response of the air/water interface stabilized by aqueous solutions of BCS and two different surfactants: the nonionic dodecyldimethylphosphine oxide (C_{12}DMPO) and the cationic dodecyltrimethylammonium bromide (DoTAB). The surface properties of both surfactants at the air−water interface have been extensively studied by different experimental methods such as tensiometry,[22,23] neutron reflectivity,[24] and excited capillary waves. The dilational viscoelastic behavior has been measured by oscillating drop profile tensiometry and by electrocapillary waves (ECW) covering together a broad frequency range.[25] The competition between proteins and surfactants at the interface will be discussed using the frequency dependence of the dilational elasticity, $\varepsilon(\omega)$, and the viscosity, $\kappa(\omega)$.

For the sake of clarity, this article is organized as follows: the materials and methods used are described in section 2. Section 3 describes briefly the theoretical background of the thermodynamic and rheological description of the protein−surfactant complex adsorption at the air/solution interface. Section 4 presents the results obtained and their discussion, and finally, section 5 the conclusions.

2. MATERIALS AND METHODS

2.1. Chemicals. The double-distilled and deionized water used for the preparation of all solutions in this work was produced by a Milli-Q-RG system from Millipore, having a resistivity higher than 18 mΩ·cm^{-1} and a surface tension of γ = 72.6 mN/m at 20 °C. Na_2HPO_4−NaH_2PO_4 buffer solution (Fluka, assay >99%) with pH 7 and surface tension of γ =72.2 mN/m at 22 °C was used to prepare the solutions of β-casein studied (3×10^{-7} and 10^{-6} M) as well as the surfactant solutions. BCS from bovine milk (purity >90%) with a molecular weight of 24 kDa and an isoelectric point of ca. pH 5.2 was purchased from Sigma-Aldrich Chemical Co. (Germany) and used without further purification. The nonionic surfactant dodecyldimethylphosphine oxide, C_{12}DMPO (M_w = 246.4 g/mol), was added to the BCS bulk solution at concentrations ranging between 10^{-6} M and the critical micelle concentration (cmc) at 5×10^{-4} M. The anionic surfactant dodecyltrimethylammonium bromide, DoTAB (M_w = 308.35 g/mol), purchased from Fluka (Switzerland), was used at concentrations ranging between 10^{-6} M and the cmc at 1.3×10^{-2} M. For lower concentrations, the signal-to-noise ratio in the ECW measurements was too low. Scheme 1 shows the molecular structure of both surfactants C_{12}DMPO and DoTAB.

Scheme 1. Chemical Structure of (a) Dodecyldimethylphosphine Oxide (C_{12}DMPO) and (b) Dodecyltrimethylammonium Bromide (DoTAB)

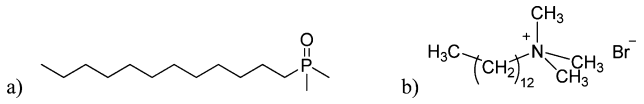

All experiments were performed at a constant temperature of 22 °C. The mixed protein−surfactant solutions were prepared mixing the respective protein and surfactant solutions 30 min before starting the measurements to ensure that the protein−surfactant complexes are fully formed. In order to ensure that the interfaces had reached the equilibrium state, surface

dx.doi.org/10.1021/jp301031y | J. Phys. Chem. B 2012, 116, 4898−4907

rheology experiments were started 2000 s after a fresh surface had been formed.[8]

2.2. Methodology. Two different experimental techniques, covering a broad range of frequencies were used for measuring the dilational viscoelastic modulus. The drop-profile analysis tensiometer PAT-1 (SINTERFACE Technologies, Germany) is suitable for measurements in the 0.01−0.2 Hz frequency range. The technique is based on the analysis of the surface tension response to controlled sinusoidal perturbations of the drop area.

The high-frequency dilational rheology was studied by the electrocapillary-wave technique, ECW, over the range of 10 Hz to 1.2 kHz. The transversal waves are excited by application of an external ac electric field (∼400 V) locally applied through a blade electrode placed right above the interface (∼750 μm). Due to the existence of different dielectric constants between both sides of the interface, the deformation follows the direction of the applied electric field. The technique has been described in detail in a previous work.[25,26] The spatial profile (u_z) of the excited electrocapillary wave is then scanned by laser reflectometry and can be described by a damped cosine function:

$$u_z(x) \approx e^{-\zeta x} \cos\left(\frac{2\pi}{\lambda}x + \phi\right) \quad (1)$$

A typical spatial profile of a excited capillary wave at a frequency ω = 400 Hz, performed as an example onto a BCS−C_{12}DMPO interfacial layer, is shown in Figure 2. It can be observed that eq 1 is able to fit very well the propagative behavior of the waves within the experimental uncertainty.

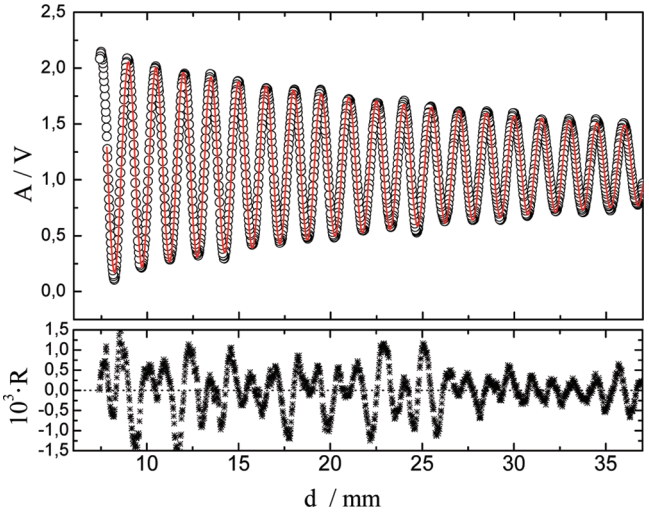

Figure 2. Spatial profile of a capillary wave generated at ω = 400 Hz on a typical BCS−C_{12}DMPO interfacial layer. (Experimental conditions: T = 22 °C, γ = 52 mN/m, [BCS] = 10^{-6}, [C_{12}DMPO] = 10^{-6} M.) Experimental data (○) were fitted to eq 1 (solid red line). The random distribution of residuals from the fit confirms the validity of the fitting equation used. A is the amplitude of the wave, d is the distance from the laser spot to the electrode, and R means residual, i.e., the difference between the experimental points and the fit.

Data analysis must be performed by the numerical solution of the dispersion relation, $D(q,\omega)$, that relates the propagation characteristics of the transversal waves (frequency ω, wavelength λ, and damping coefficient ζ) to the constitutive parameters of the monolayer (surface tension γ, dilational elasticity ε, and viscosity κ).[27,28] $D(q,\omega)$ is given by

$$D(q, \omega) = T(q, \omega; \gamma)L(q, \omega; \varepsilon^*) + C(q, \omega) = 0 \quad (2)$$

where $T(\gamma,q,\omega)$ accounts for the capillary contribution, $L(\varepsilon^*,q,\omega)$ for the dilatational one, and $C(q,\omega)$ for the coupling term. This relation allows obtaining information on the dilational moduli, ε and $\omega\kappa$, from measurements of the propagation parameters of the excited waves. The three terms of the dispersion equation are given by

$$T(q, \omega, \gamma) = \left[\gamma q^2 + i\eta_1\omega(q + m_1) + i\eta_2\omega(q + m_2) - \frac{(\rho_1 + \rho_2)\omega^2}{q}\right]$$

$$L(q, \omega, \tilde{\varepsilon}) = [\tilde{\varepsilon}(\omega)q^2 + i\eta_1\omega(q + m_1) + i\eta_2\omega(q + m_2)]$$

$$C(q, \omega) = [\eta_1\omega(q - m_1) - \eta_2\omega(q - m_2)]^2 \quad (3)$$

where q is the complex wave vector, γ is the surface tension, and ε^* is the dilational complex elasticity modulus. ρ_i and η_i are the density and viscosity of water (i = 1) and air (i = 2), respectively, and $m_i = (q^2 - i\omega\rho_i/\eta_i)^{1/2}$ is the inverse penetration depth.

3. THEORETICAL BACKGROUND

Dilational rheology explores the surface tension response to dilational deformations (compression and/or expansion) of the adsorbed layer at fluid/fluid interfaces. The surface complex elastic modulus $\varepsilon^*(\omega)$ is related to the change of surface tension γ for a small increase of surface area A according to[29]

$$\varepsilon^*(\omega) = \frac{\mathcal{I}\{\Delta\gamma(t)\}}{\mathcal{I}\{\Delta A(t)/A_0\}} = \frac{\mathcal{I}\left\{\frac{d\Delta\gamma(t)}{dt}\right\}}{\mathcal{I}\left\{\frac{d\ln A(t)}{dt}\right\}} \quad (4)$$

where $\mathcal{I}$ denotes Fourier transform and γ is the surface tension. The viscoelastic modulus ε^* is a frequency-dependent complex quantity.[28,30]

$$\varepsilon^*(\omega) = \varepsilon(\omega) + i\varepsilon''(\omega) = \varepsilon(\omega) + i\omega\kappa(\omega) \quad (5)$$

where $\varepsilon(\omega)$ is the storage term that accounts for the elastic energy, $\varepsilon''(\omega)$ accounts for the energy dissipated, and κ is the dilational viscosity.

A first model accounting for the dilational viscoelastic modulus of a surface layer of a surfactant was proposed by Lucassen and van den Tempel, the LVT model, assuming a diffusion-controlled exchange of matter mechanism:[20]

$$\varepsilon^*(\omega) = \varepsilon_0\left(\frac{d\Gamma}{dC}\sqrt{\frac{i\omega}{D}}\right)\Big/\left(1 + \frac{d\Gamma}{dC}\sqrt{\frac{i\omega}{D}}\right) = \frac{1 + \zeta + i\zeta}{1 + 2\zeta + 2\zeta^2} \quad (6)$$

where the surface dilational elasticity ε_0 is the high-frequency limit, and the characteristic parameters of the diffusional exchange of matter between bulk and surface, ζ and ω, are given by $\varepsilon_0 = d\Pi/d\ln\Gamma$, $\zeta = (\omega_D/\omega)^{1/2}$, and $\omega_D = (D/2)(dC/d\Gamma)^2$. Γ represents the surfactant adsorption at the interface, Π the surface pressure, and C is the bulk concentration.

dx.doi.org/10.1021/jp301031y | J. Phys. Chem. B 2012, 116, 4898−4907

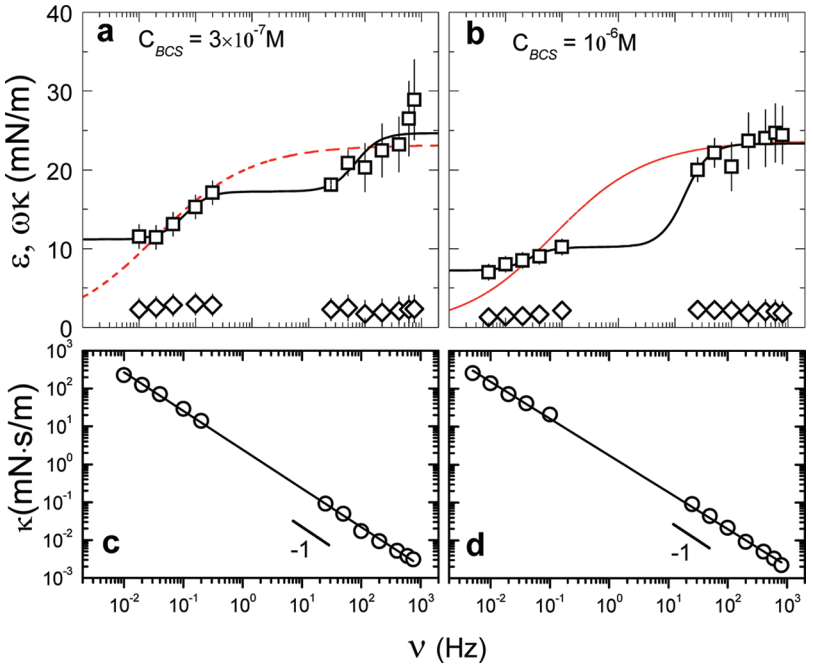

Figure 3. Frequency dependence of the dilational elastic modulus, ε (□), the loss modulus, $\omega\kappa$ (◇), and the dilational viscosity κ (○) of the air/BSC solution interface. Two different BCS concentrations, 3×10^{-7} (a, c) and 10^{-6} M (b, d), have been measured. The red lines represent the fit of the experimental data to a single LVT model (eq 6), while the continuous black ones correspond to the sum of a LVT and a Maxwell mode (eq 7).

Recently, the LVT model was extended taking into account the existence of a first-order kinetic process that may be superposed to the diffusional exchange assumed by LVT.[31] Indeed, this kinetic process can account for an internal reorganization of the adsorption layer via different processes such as phase transitions, molecular reorientation, etc.[32,33]

Assuming the existence of consecutive linear kinetic processes and excluding any diffusional mechanism, i.e., considering the layer as insoluble, the frequency dependence of ε^* may be described by the sum of j−Maxwell relaxation modes[34]

$$\varepsilon^*(\omega) = \varepsilon(\omega) + i\omega\kappa = \sum_{k=1,2} \frac{\varepsilon_{0,k}\omega\tau_k}{1 + i\omega\tau_k} \tag{7}$$

where τ_k is the relaxation time of the kth kinetic process. $\varepsilon_{0,k}$ accounts for the equilibrium elasticity for the k relaxation mode. The existence of more than one Maxwell mode was already used to describe the elasticity of polymer monolayers at the air/water interface.[26,35]

For mixed protein−surfactant adsorption layers, the relation describing ε^* takes into account the diffusion coefficients and relevant thermodynamic parameters related to all the components.[19] The general expressions were adopted to mixtures of two surfactants with the surface tension $\gamma = \gamma(\Gamma_1,\Gamma_2,T)$ and with the adsorption of each component $\Gamma_j = \Gamma_j(C_{s_1},C_{s_2})$, where Γ_j is the adsorption of species j, and the C_{s_j} are the subsurface concentrations of component j in the mixture. Assuming a diffusion-controlled mechanism for the adsorption layer relaxation, the following mass balance equation results, which is valid for harmonic oscillations at a frequency ω and a small area amplitude ΔA:

$$i\omega\Delta\Gamma_j + i\omega\Delta\Gamma_j\frac{\Delta A}{A} + (i\omega D_j)^{1/2}\Delta C_{s_j} = 0 \tag{8}$$

where D_j is the diffusion coefficient of component j. Equation 9 yields the complex viscoelasticity of a mixed layer:[18]

$$\varepsilon = \frac{1}{B}\left(\frac{\partial\Pi}{\partial \ln\Gamma_1}\right)_{\Gamma_2}\left[\sqrt{\frac{i\omega}{D_1}}a_{11} + \sqrt{\frac{i\omega}{D_2}}a_{12}\frac{\Gamma_2}{\Gamma_1} + \frac{i\omega}{\sqrt{D_1D_2}}(a_{11}a_{22} - a_{12}a_{21})\right] + \frac{1}{B}\left(\frac{\partial\Pi}{\partial \ln\Gamma_2}\right)_{\Gamma_1}\left[\sqrt{\frac{i\omega}{D_1}}a_{21}\frac{\Gamma_1}{\Gamma_2} + \sqrt{\frac{i\omega}{D_2}}a_{22} + \frac{i\omega}{\sqrt{D_1D_2}}(a_{11}a_{22} - a_{12}a_{21})\right] \tag{9}$$

where C_1 and C_2 are the bulk concentrations of the components and $a_{ij} = (\partial\Gamma_i/\partial C_j)|c_{k\neq j}$ are the partial derivatives to be determined from the adsorption isotherm. The coefficient B depends on the mechanism for the adsorption dynamics of the interfacial layer. For two components, only adsorption and desorption process are assumed both controlled by diffusion; thus, B is given by

$$B = 1 + \sqrt{\frac{i\omega}{D_1}}a_{11} + \sqrt{\frac{i\omega}{D_2}}a_{22} + \frac{i\omega}{\sqrt{D_1D_2}}(a_{11}a_{22} - a_{12}a_{21}) \tag{10}$$

This model has been used to discuss the competitive adsorption of complexes of proteins and surfactants at liquid/air interfaces. To determine the dilational moduli from the above model, it is necessary to use a model for predicting the equilibrium surface adsorption layer obeying the correspondent equations of state and adsorption isotherms.

dx.doi.org/10.1021/jp301031y | J. Phys. Chem. B 2012, 116, 4898−4907

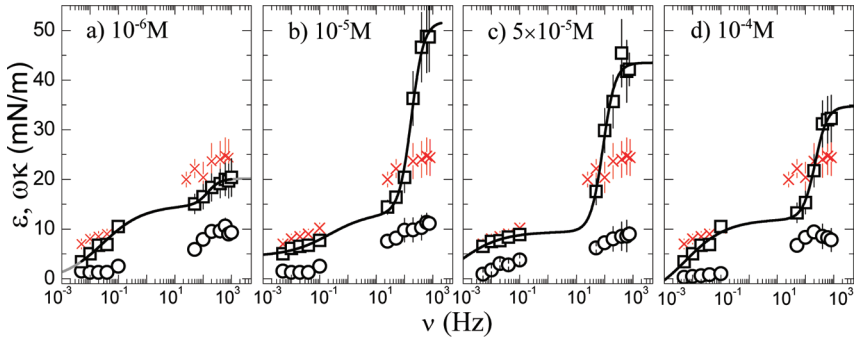

Figure 4. Frequency dependence of the dilational elastic module ε (□) and the loss module $\omega\kappa$ (○) for BCS−C_{12}DMPO adsorbed layers at the air−water interface, measured for different C_{12}DMPO bulk concentrations (indicated inside the figures) at a fixed protein concentration of 10^{-6} M. For the sake of comparison, elasticity data from Figure 3 corresponding to BCS at the same concentration has been added (×). Continuous lines represent the fit of the BCS−C_{12}DMPO data to a LVT+Maxwell model.

For mixtures of a protein and a nonionic surfactant, the following equation of state of the surface layer was proposed some years ago:[9,36]

$$\frac{-\Pi\Omega_0^*}{RT} = \ln(1 - \theta_P - \theta_S) + \theta_P(1 - \Omega_0/\Omega_P) + a_P\theta_P^2 + a_S\theta_S^2 + 2a_{PS}\theta_P\theta_S \quad (11)$$

where the subscripts P and S refer to the protein and surfactant molecules, respectively. Π is the surface pressure, R is the gas constant, and T is the absolute temperature. Γ_i, Ω_i, and a_i are the adsorption, average molar area, and interaction constant for the component i, respectively. $\theta_i = \Omega_i\Gamma_i$ is the surface coverage by surfactant molecules of component i, Ω_0^* is the average molar area of the protein + surfactant, and Ω_0 is the molar area at zero surface pressure. The parameter a_{PS} accounts for the interaction between the protein and surfactant molecules.

The adsorption behavior of a protein mixed with an ionic surfactant is rather different. For a protein molecule with m-ionized groups, the Coulomb interaction with ionic surfactants causes the formation of complexes, which are determined by the average activity of ions $(c_P{}^m c_S)^{1/(1+m)}$. The resulting equation of state of the surface layer is similar to eq 11:

$$\frac{-\Pi\Omega_0^*}{RT} = \ln(1 - \theta_{PS} - \theta_S) + \theta_{PS}(1 - \Omega_0/\Omega_P) + a_{PS}\theta_{PS}^2 + a_S\theta_S^2 + 2a_{SPS}\theta_{PS}\theta_S \quad (12)$$

where $\theta_{PS} = \Omega\Gamma$ is the coverage of the interface by adsorbed protein−surfactant complexes and a_{SPS} is the parameter which describes the interaction of the not associated surfactant with the protein−surfactant complexes. It was shown that the assumption of an intrinsic compressibility of surfactant, $\Omega_S = \Omega_{S0}(1 - \varepsilon_S\Pi\theta_S)$, improves the quality of the model to describe the experimental data. Here, Ω_{S0} ($\Omega_0 \approx \Omega_{S0}$) is the molar area of surfactant at zero surface pressure and ε_S is the two-dimensional relative surface layer compressibility of the surfactant molecules in the surface layer. The influence of aggregation was taken into account in the theory in an approximated way by introducing a difference of the average molar area of adsorbed molecules. It is clear at this point that other complex phenomena related to protein surface layers remain far from the possibilities of a quantitative description by this thermodynamic model. This general picture of the equilibrium adsorption of mixed adsorption layers has been described in detail in ref 9. It has to be remarked that, in the papers published so far, the parameters of the above model have been obtained using experimental data of dynamic and equilibrium surface tension, and of low-frequency surface rheology. Even though the high-frequency behavior of the dilational elasticity and viscosity has been predicted, no direct comparison between the theoretical predictions and experimental data has been done at high frequencies.

4. RESULTS AND DISCUSSION

4.1. Interfacial Rheology of β-casein Film. Figure 3, a and b, shows the frequency dependence of ε' and ε'', for two different bulk concentrations of β-casein (3×10^{-7} and 10^{-6} M), close to the critical region of concentration ($c^* = 4 \times 10^{-7}$ M), where the adsorption layer is saturated by BCS molecules, and where the formation of a second layer of surface aggregates is formed.[36] Two well-defined relaxation processes are clearly visible, and the values of storage modulus are much larger than the loss ones ($\varepsilon' \gg \omega\kappa$) over most of the frequency range, thus pointing out that the system does not have enough time to dissipate energy by relaxation, and therefore the surface behaves mainly as an elastic body. For frequencies below 0.1 Hz the viscous dissipation effects cannot be neglected. The surface elasticity modulus of a BCS solution close to the critical region of concentration ($c^* \approx 3 \times 10^{-7}$ M) is slightly larger than for another one just above it (10^{-6} M). It has already been shown in the literature that the elasticity of the BCS layers shows a maximum near the transition from a monolayer to a multilayer, where new energy dissipation mechanisms exist.[37] This can also explain why the low-frequency relaxation process seems to be shifted to lower frequencies for the 10^{-6} M solution. In fact, the elasticity increases very little for this concentration, and therefore the uncertainties of the LVT parameters for this process are rather large. The frequency dependence of the dilational viscosity κ at both protein concentrations (Figure 3, c and d) can be described by a power law over the whole frequency range: $\kappa \sim \omega^{-f}$, with $f \approx 1.0 \pm 0.1$, thus showing a behavior given by Amonton's law ($f = 1$), as already found for some Langmuir polymer monolayers.[35]

In the next section we will describe the surface dilational response of BCS−surfactant solutions with a constant protein concentration close to the precritical region, [BCS] = 10^{-6} M, and increasing amounts of added surfactant.

4.2. Interfacial Rheology of BCS/Surfactant Interfacial Systems. *4.2.1. BCS−C_{12}DMPO Adsorption Layers.* Figure 4 shows the frequency dependence of ε' and $\varepsilon'' = \omega\kappa$ of BCS−C_{12}DMPO interfacial layers over a broad surfactant concen-

dx.doi.org/10.1021/jp301031y | J. Phys. Chem. B 2012, 116, 4898−4907

tration range below the surfactant cmc (from 10^{-6} to 10^{-4} M) at a fixed protein concentration of 10^{-6} M. Also, the corresponding results for solutions of pure BCS are included (data from Figure 3). As in the case of pure BCS at the interface, the values of ε' are larger than $\varepsilon'' = \omega\kappa$ over the whole frequency range considered, in agreement with the picture that the interfacial layer behaves as a mainly elastic body for frequencies above 0.1 Hz. The elasticity shows a maximum value at intermediate surfactant concentrations ($\approx 10^{-5}$ M) as shown in Figure 5b, whereas the high-frequency loss modulus—higher than for the BCS solutions—shows a weak concentration dependence. At low frequencies ε increases because the nonionic surfactant coadsorbs, thus increasing the total surface concentration. Above a threshold bulk concentration, the surfactant displaces the protein from the interface, which reduces the elastic modulus, thus leading to the appearance of a maximum. Note that BCS−C_{12}DMPO interfacial layers and the ones of pure BCS present comparable values of ε' in the low-frequency range (Figure 4), independent of the surfactant concentration, while in the high-frequency regime, the BCS + C_{12}DMPO system has values of ε' significantly higher than for the BCS solutions above 100 Hz except for [C_{12}DMPO] = 10^6 M, whereas one finds the opposite below that frequency. Following Gao et al.,[37] this could be explained by the depletion of the protein segments—mainly loops and tails—adsorbed at the interface via the hydrophobic interaction with C_{12}DMPO molecules. The higher hydrophobicity of the BCS−C_{12}DMPO complex would justify the fact that ε is significantly higher for the complex than for the pure BCS solutions over most of the surfactant concentration range.

Assuming that hydrophobic segments of the BCS molecules are irreversibly adsorbed at the air/water interface, it is possible to fit the frequency dependence of the dilational elasticity corresponding to the BCS−C_{12}DMPO complex within the experimental uncertainty using a LVT and a consecutive Maxwell process as for the pure BCS solutions (continuous lines in Figure 4).

To explain the qualitative trends of the results found for BCS + C_{12}DMPO, one can consider that there exists a replacement of BCS by surfactant at the interfacial layer as the C_{12}DMPO concentration increases. This scenario was previously suggested by Kotsmar et al.[36] to explain their dynamic surface tension experiments and is schematically shown in Figure 1. It is well-known that during the initial steps of adsorption mainly surfactant molecules adsorb due to their higher diffusion coefficient. After that, the surface concentration of the complex increases gradually, thus increasing the surface elasticity. At relatively high surfactant concentrations, it is expected that the structure of the protein−surfactant complex changes, which means that the complexes are formed due to hydrophobic interactions of the nonionic C_{12}DMPO with the BCS molecules (according to the scheme of Figure 1). Consequently, the increase of surfactant molecules modifies the adsorption layer structure, thus leading to a change of the surface tension as well as the dilational elasticity (Figure 5).[9] Note that at concentrations close to 5×10^{-5} M the values of γ corresponding to the complex layer are comparable to the ones corresponding to the pure surfactant at the interface supporting the assumed replacement of the BCS molecules due to its interaction with the surfactant molecules via hydrophobic interaction.

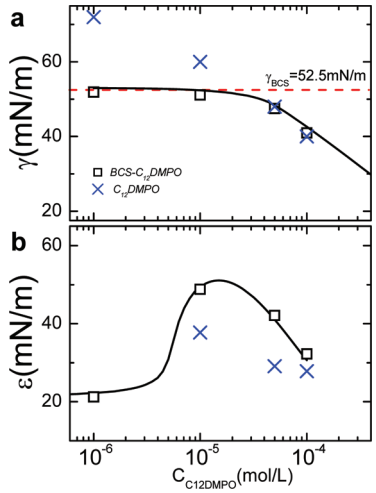

Figure 5. Surface tension γ (a), and dilational elastic module ε' (b) for BCS−C_{12}DMPO adsorbed layers at 800 Hz as a function of C_{12}DMPO concentration. Also included are the parameters γ and ε' of pure C_{12}DMPO adsorbed layers. The continuous lines correspond to the theoretical model described by eqs 11 and 12 using the parameters given in Table 1. The protein concentration was 10^{-6} M in all the cases.

As can be seen in Figure 4, the slight decrease in the dilational module ε from $C = 5 \times 10^{-5}$ M is caused by the increasing amount of surfactant. Therefore, in this concentration regime the surfactant dominates the interfacial layer, in agreement with results previously reported using different techniques.[36] Further increase of nonionic surfactant concentration increases the number of free surfactants molecules, which leads to a stronger competition at the interface. Both effects lead finally to a progressive depletion of the protein from the interface decreasing ε as can be seen in Figure 5b. This figure also shows the predictions of the theoretical model previously discussed (see Theoretical Background section) for BCS + C_{12}DMPO at a constant frequency (800 Hz) and using the parameters of Table 1 taken from ref 9. These predictions,

Table 1. Parameters of the Model Given in Ref 8 Used for Predicting the Experimental Adsorption Data for BCS−C_{12}DMPO Mixture

	Ω_0 (10^5 m^2/mol)	Ω_1 (10^6 m^2/mol)	Ω_{max} (10^7 m^2/mol)	a_{PS}	b_P (m^3/mol)
BCS	2.2	3.0	2.7	1.1	1.0×10^2
	Ω_{S0} (10^5 m^2/mol)	a_S	a_{SPS}	ε_S (10^{-3} m/mN)	b_S (m^3/mol)
C_{12}DMPO	2.5	0.0	0.0	9.0	1.96×10^2

including the ones corresponding to other frequencies (results not shown), agree very well with the experimental data, and describe well the maximum in the dilational elastic module ε'. However, this is not sufficient for understanding the complex behavior of the mixed adsorption layers, but it is also necessary to take into account additional effects accounting for other processes, such as molecular reconformation, aggregation, disaggregation, etc. Note that any change in ε' can be explained by two effects: the relaxation of bound surfactants, which can be released upon expansion and rebound upon compression during the propagation of a longitudinal wave onto the interface,[36] and the relaxation of the segments of BCS attached at the air/water interface.[18]

dx.doi.org/10.1021/jp301031y | J. Phys. Chem. B 2012, 116, 4898−4907

Figure 6 shows the relation of ε on the frequency ν, at two surfactant concentrations for BCS−C_{12}DMPO interfacial

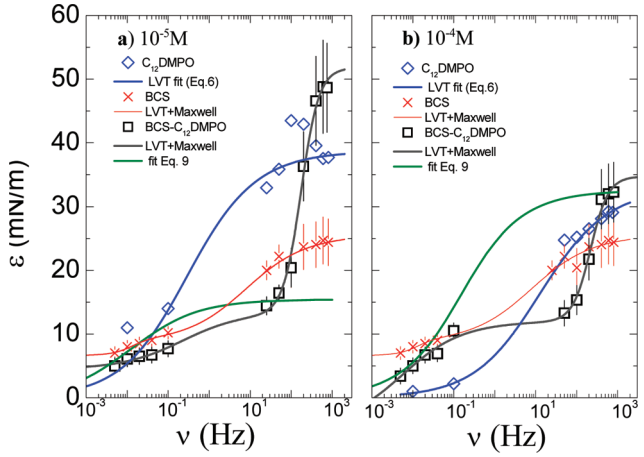

Figure 6. Elasticity modulus as a function of the frequency of the protein−surfactant complex, the pure protein, and the pure surfactant at the air/water interface at two different C_{12}DMPO concentrations: (a) 10^{-5} M and (b) 10^{-4} M. The fits and predictions from the different theoretical models (see inset of the figures and text) have been included. The parameters of the fits to eq 9 are given in Table 1.

complex layers, pure BCS, and pure C_{12}DMPO, as well as the predictions by the given model. In addition to the comparison of the elasticity of the complex and of pure BCS done above, Figure 6 shows that above 300 Hz the elasticity of the complex is higher than that of the pure surfactant, while the opposite is true between 10 and 300 Hz. The low-frequency behavior is strongly dependent on the surfactant concentration, even though the two concentrations shown are below the cmc of the surfactant. The same is true when the elasticities of the complex and of C_{12}DMPO are compared, although where the two $\varepsilon(\omega)$ curves cross each other is slightly higher than in the case of the BCS solution. This points out that at high frequencies there is a fundamental difference between relaxation mechanisms of the complex, the protein, and the surfactant that makes the relaxation much faster for the protein + surfactant equilibrium mixture. Since the hydrophobization of the protein by the surfactant decreases the contribution of the dynamics of the adsorption/desorption of short trains of amino acids,[37] the most plausible mechanism may be the complex ↔ protein + surfactant in the surface layer. As previously shown in Figures 3 and 4, the dilational elasticity of pure BCS layers can be roughly described using a model based on the consecutive LVT + Maxwell processes similarly to the case of the complex BCS−C_{12}DMPO, independently of the surfactant concentration. However, the model given by the eqs 9 and 10 does not describe properly the elasticity at high frequencies. This may be due to additional relaxation processes for the surfactant molecules that are not taken into account in this theoretical model. Furthermore, the behavior of the pure interfacial layers of C_{12}DMPO can be described in terms of the LVT model except for the lowest frequencies. Even though the LVT model has been commonly used to described the adsorption of nonionic surfactants,[19] it was already found that even a more sophisticated model including in-plane compressibility of the monolayer was not completely satisfactory for this surfactant.[38]

4.2.2. BCS−DoTAB Adsorption Layers. In this section, we describe the surface behavior of the BCS−DoTAB system at different surfactant concentrations (from 10^{-4} to 10^{-2} M). Note that the cmc of DoTAB is 1.3×10^{-2} M and that the fixed protein concentration (10^{-6} M) is just above the critical concentration at which a secondary layer starts to be formed. Figure 7a shows the surfactant concentration dependence of

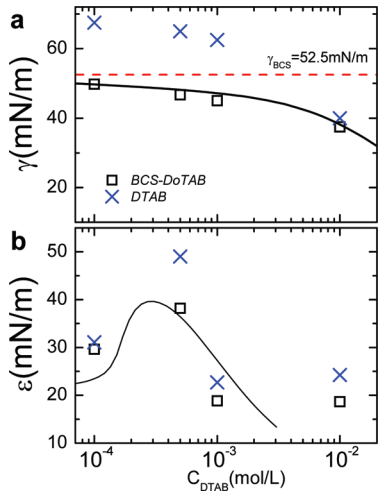

Figure 7. Surface tension γ (a) and dilational elastic module ε' (b) for BCS−DoTAB adsorbed layers at 800 Hz as a function of DoTAB concentration, and for [β-casein] = 10^{-6} M. Also included are the data of γ and ε for pure DoTAB adsorbed layers. The solid line corresponds to the theoretical model described in eqs 9−12, with the parameters shown in Table 2.

the surface tension of CTAB and BCS + DoTAB solutions at constant BCS concentration. Contrary to the BCS + C_{12}DMPO system (Figure 5), the formed complex increases the hydrophobicity of the protein, i.e., its surface activity. This type of effect has been frequently described for solutions of opposite charged polyelectrolytes and surfactants, and has been attributed also to the fact that the complex becomes more hydrophobic as the surfactant concentration increases.[39] The results of Figure 7a suggest that for $10^{-4} < C/\mathrm{M} < 10^{-2}$ both BCS-DoTAB and $DoTA^+$ adsorb at the air/water interface and that for $C > 10^{-2}$ M the BCS molecules are displaced from the surface. The absence of a maximum in the γ versus C curve and no precipitates in the solutions exclude any coacervation process in the concentration range studied.[40]

Figure 8 shows the frequency dependence of ε and $\omega\kappa$. The qualitative trends are similar to those of Figure 4, and at high frequencies the surface behaves as a mainly elastic layer. Indeed, the shape of the experimental curves is qualitatively similar to those of pure DoTAB solutions (Figure 9). While below 1 Hz the elasticity of the pure BCS solution is slightly higher than that of the complex, the behavior at high frequencies depends on the surfactant concentration: below $C = 5 \times 10^{-4}$ M the elasticity of the complex is lower than that of BCS, and above that concentration the behavior is the opposite.

It is well-known that ionic surfactants, such as DoTAB, hydrophobize the protein in the low surfactant concentration range due to the neutralization of part of the charges (and also to hydrophobic interactions). As a consequence, the complex attaches to the surface to the interface even stronger than in the case of the complex formed by the protein and nonionic surfactants.[36] As expected from the elasticity data plotted on the Figure 7b, as the total concentration of surfactant increases, the elasticity increases due to the increasing amount of bound

dx.doi.org/10.1021/jp301031y | J. Phys. Chem. B 2012, 116, 4898−4907

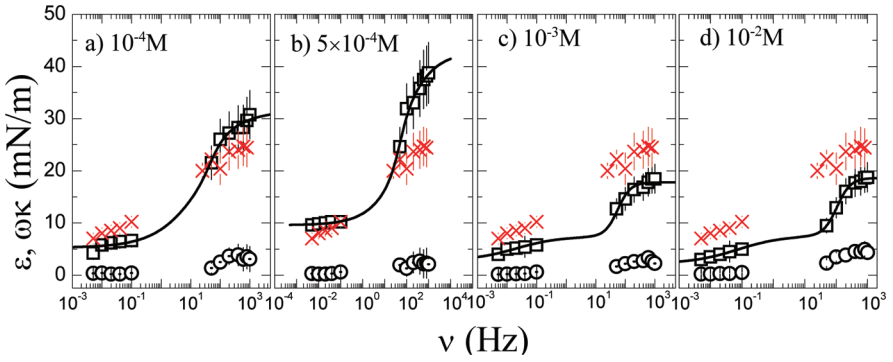

Figure 8. Frequency dependence of the dilational elastic module ε (□) and the loss module $\omega\kappa$ (○) for BCS−DoTAB adsorbed layers. The figures correspond to four surfactant concentrations (indicated in the labels), and at fixed protein concentration (10^{-6} M). For the sake of comparison, elasticity data from Figure 3 corresponding to BCS at the same concentration have been added (×). Solid lines represent the fit to the LVT+Maxwell model.

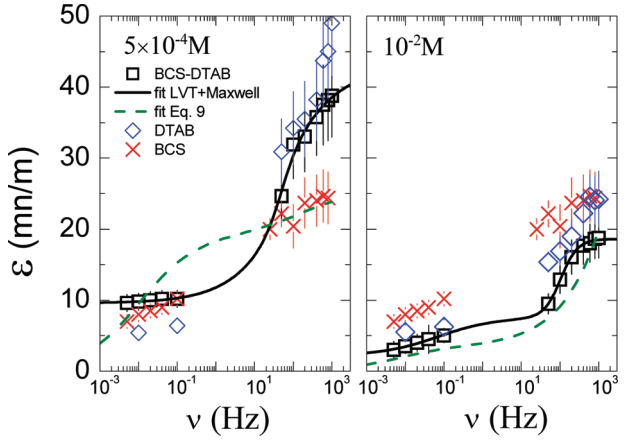

Figure 9. Frequency dependence of the dilational elastic module ε (□) and the loss module $\omega\kappa$ (○) for BCS-DoTAB adsorbed layers. The figures correspond to four surfactant concentrations (indicated in the labels), and at fixed protein concentration (10^{-6} M). For the sake of comparison, elasticity data from Figure 3 corresponding to BCS at the same concentration have been added (×), as well as the data corresponding to pure DoTAB (◇). Continuous black lines represent the fit to a LVT+Maxwell model, and the green lines to the predictions of the model given by eqs 9 to 12 using the parameters given in Table 2.

surfactant to a maximum value at 5×10^{-4} M; the subsequent decrease is caused by the increasing amount of free surfactant and hence enhanced exchange of surfactant molecules between the surface and the bulk. An inspection of Figure 8 clearly shows that the maximum observed in Figure 7b is found over the whole 50 Hz to 1 kHz range. Figure 7b also includes the predictions of the theoretical model previously used for the BCS−C_{12}DMPO system. The parameters taken from ref 9 are given in Table 2 and were not fitted to the data presented in this work. The model roughly predicts the maximum of ε, while the ability of the model to describe the behavior of the complete set of data is poor as compared to that found for the BCS−C_{12}DMPO system. More specifically, the theory strongly underestimates the experimental results at high DoTAB concentrations, which can be due to the fact that the theory does not takes into account properly the depletion of the protein from the surface due to the interaction with the surfactants. For mixed solutions of lysozyme and SDS it was shown by Alahverdjieva et al.[41] that the experimental isotherm data shift from a dependence driven by ionic interaction to one

Table 2. Parameters of the Model Given in Ref 8 Used for Predicting the Experimental Adsorption Data for BCS−DoTAB Mixture

	Ω_0 (10^5 m^2/mol)	Ω_1 (10^6 m^2/mol)	Ω_{max} (10^7 m^2/mol)	a_{PS}	b_P (m^3/mol)
BCS	2.2	3.0	2.7	1.1	1.0×10^2
	Ω_{S0} (10^5 m^2/mol)	a_S	a_{SPS}	ε_S (10^{-3} m/mN)	b_S (m^3/mol)
DoTAB	2.1	0.0	0.0	8.0	1.2×10^2

obtained for a model based on a pure competitive adsorption of the two compounds. For the dilation viscoelasticity, such model calculations are not available yet.

A comparison of the high-frequency behavior of the elasticity of the BCS−C_{12}DMPO and BCS−DoTAB systems (Figures 4 and 8) shows a qualitatively similar behavior except for the fact that in the case of the ionic surfactant the complex is less elastic than pure BCS at high surfactant concentrations. The main difference with respect to the complex with C_{12}DMPO is the ability of the surfactant to hydrophilize the protein at high surfactant concentrations, which might enhance the contribution of short trains of amino acid residues to dissipate energy by adsorbing and desorbing from the layer, as suggested by Gao et al.[37]

The given picture is in general agreement with earlier studies of Mackie et al., who assumed the existence of a competitive adsorption of both surfactant and complex at lower surfactant concentrations followed by a displacement of the protein by the surfactant at higher concentrations.[42−44] However, the orogenic displacement mechanism of protein−surfactant complex by surfactant, discussed in the papers by Mackie,[42] must go along with a molecular hydrophilization via hydrophobic interaction with surfactant molecules as suggested previously by Kotsmar et al.[9]

Figure 9 highlights the different theoretical approaches presently available for the description of not only the BCS−DoTAB interfacial complex layers, but also of pure BCS as well C_{12}DMPO at the air/water interface. As was previously demonstrated, the dilational elasticity of pure BCS layers can be roughly described using a model based on the consecutive LVT + Maxwell processes similarly to the case of the complex BCS−DoTAB, independently of the surfactant concentration. However, the model derived to describe the equilibrium adsorption behavior does not allow modeling the elasticity at high frequencies, which can be explained in the context of the

dx.doi.org/10.1021/jp301031y | J. Phys. Chem. B 2012, 116, 4898−4907

different dissipation mechanisms discussed above, and not taken into account by the theory. Further, as it can be expected the behavior of the pure interfacial layers of C_{12}DMPO can be expressed in terms of the LVT model, which is commonly used to described the adsorption of nonionic surfactants.[20]

As a final remark, we have found larger values of the dilational elastic module for mixtures with C_{12}DMPO as compared to DoTAB in the whole surfactant concentration regime shown by Figures 5 and 7. Several factors may contribute to this behavior. (a) On one hand, for a given surfactant concentration, C_{12}DMPO is much more surface active than DoTAB, which is very important for the surface elasticity and viscosity of layers that contain significant amounts of surfactants (alone or in competition in a mixed surface layer). At constant frequency and the same number of surfactant molecules, the elasticity is higher for a surfactant that adsorbed at the lower bulk concentration, i.e., for the more surface active surfactant. This higher surfactant concentration leads to a higher compression of the protein layer, thus leading to a more elastic surface film. (b) On the other hand, the adsorbed surfactants can lead to changes in the structure of the BCS segments attached at the air/water interface due to the complex formation. The structure of the complexes may be different for the two surfactants because of the interaction with different surfactant molecules: hydrophobic interactions in the case of C_{12}DMPO, and electrostatic and hydrophobic in the case of DoTAB.

In addition to the comparison of the elasticity of the complex and pure BCS made above, it can be observed that above 50 Hz and for surfactant concentrations close to the cmc, the elasticity of the complex is slightly lower than that of the surfactant and lower than that of BCS. However, for low surfactant concentrations both the complex and the surfactant have very similar elasticities, substantially higher than that of BCS. This behavior is almost the opposite to the one observed below 1 Hz.

5. CONCLUSIONS

The dilational viscoelastic behavior of BCS−C_{12}DMPO and BCS−DoTAB adsorption layers at the air−water interface has been investigated by the combination of the drop profile analysis tensiometry in the low-frequency range and excited capillary waves in the high-frequency domain. Previous experiments performed by other authors,[36] which study the adsorption isotherms of the single components and the mixtures, suggest that the BCS molecules can be displaced from the surface by the surfactant molecules. The dilational rheology studied in this work confirms these findings. The interfacial dynamical experiments show that the composition of the layers can differ depending on the surfactant concentration and nature. Our results suggest that for both BCS−surfactant complexes the characteristics of the mixed layers are essentially corresponding to a competitive adsorption mechanism. Hence, we have demonstrated that further increase of the surfactant concentration results in a decrease of the viscoelastic module values indicating the successive protein displacement. It is remarkable that the different values found for both surfactants, in the whole surfactant concentration range, are mainly higher in mixtures with C_{12}DMPO as compared to those with DoTAB. Indeed, probably C_{12}DMPO displaces the protein molecules more efficiently from the surface, which correlates to its higher surface activity as compared to DoTAB. This fact could be due to small changes in the structure of the BCS caused by the interaction with the surfactants because C_{12}DMPO interacts more efficiently with BCS than DoTAB.

We have used a theoretical model previously published by other authors (ref 8) for a quantitative description of the dilational rheology of the surface layers of single components and their mixtures. There is some mismatch between the experimental results and the theoretical curves for the dilational rheology in the region of interfacial competition. This can be explained by the fact that the theory requires refinement in order to better account for the particular interfacial properties of the protein−surfactant complexes in this concentration range, i.e., to better describe the transition from an ionic interaction to a purely hydrophobic interaction for the BCS−DoTAB mixed adsorption layer.

AUTHOR INFORMATION

Present Address

[⊥]Laboratoire de Physique des Solides, Bâtiment 510,Université Paris-Sud XI, 91405-Orsay, France.

Notes

The authors declare no competing financial interest.

REFERENCES

(1) Dickinson, E.; Walstra, P. *Food Colloids and Polymers: Stability and Mechanical Properties*; Royal Society of Chemistry: Cambridge, UK, 1993.
(2) Lalchev, Z. I.; Todorov, R. K.; Christova, Y. T.; Wilde, P. J.; Mackie, A. R.; Clark, D. C. *Biophys. J.* **1996**, *71*, 2591−260.
(3) Miller, R.; Fainerman, V. B.; Makievski, A. V.; Kragel, J.; Grigoriev, D. O.; Kazakov, V. N.; Sinyachenko., O. V. *Adv. Colloid Interface Sci.* **2000**, *86*, 39−82.
(4) Ladha, S.; Mackie, A. R.; Harvey, L. J.; Clark, D. C.; Lea, E. J. A.; Brullemans, M.; Duclohier, H. *Biophys. J.* **1996**, *71*, 1364−1373.
(5) Giffard, C. J.; Ladha, S.; Mackie, A. R.; Clark, D. C.; Sanders, D. *J. Membr. Biol.* **1996**, *151*, 293−300.
(6) Aksenenko, E. V.; Kovalchuk, V. I.; Fainerman, V. B.; Miller, R. *J. Phys. Chem. C* **2007**, *111*, 14713−14719.
(7) Erni, P.; Fischer, P.; Herle, V.; Haug, M.; Windhab, E. J. *Chem. Phys. Chem* **2008**, *9*, 1833−1837.
(8) Erni, P.; Fischer, P.; Heyer, P.; Windhab, E. J.; Kusnezov, V.; Lauger, J. *Prog. Colloid Polym. Sci. S* **2004**, *129*, 16−23.
(9) Kotsmar, C.; Pradines, V.; Alahverdjieva, V. S.; Aksenenko, E. V.; Fainerman, V. B.; Kovalchuk, V. I.; Krägel, J.; Leser, M. E.; Noskov, B. A.; Miller, R. *Adv. Colloid Interface Sci.* **2009**, *150*, 41−54.
(10) Maldonado-Valderrama, J.; Martin-Molina, A.; Martin-Rodriguez, A.; Cabrerizo-Vilchez, M. A.; Galvez-Ruiz, M. J.; Langevin, D. *J. Phys. Chem. C* **2007**, *111*, 2715−2723.
(11) Noskov, B. A.; Latnikova, A. V.; Lin, S. Y.; Loglio, G.; Miller, R. *J. Phys. Chem. C* **2007**, *111*, 16895−16901.
(12) Graham, D. E.; Phillips, M. C. *J. Colloid Interface Sci.* **1979**, *70*, 403−414.
(13) de Feitjer, J. A.; Benjamins, J. In *Food Emulsions and Foams*; Dickinson, E., Ed.; The Royal Society of Chemistry: London, 1987.
(14) Beverung, C. J.; Radke, C. J.; Blanch, H. W. *Biophys. Chem.* **1999**, *81*, 59−80.
(15) Dickinson, E.; Matsumura, Y. *Colloids Surf. B* **1994**, *3*, 1−17.
(16) van Vliet, T.; Martin, A. H.; M. A. Bos, M. A. *Curr. Opin. Colloid Interface Sci.* **2002**, *7*, 462−468.
(17) Freer, E. M.; Yim, K. S.; Fuller, G.; Radke, C. J. *J. Phys. Chem. B* **2004**, *108*, 3835−3844.
(18) Miller, R.; Fainerman, V. B.; Leser, M. E.; Michel, M. *Curr. Opin. Colloid Interface Sci.* **2004**, *9*, 350−356.
(19) Aksenenko, E. V.; Kovalchuk, V. I.; Fainerman, V. B.; Miller, R. *J. Phys. Chem. C* **2007**, *111*, 14713−14719.
(20) Lucassen, J.; van den Tempel, M. *Chem. Eng. Sci.* **1972**, *27*, 1283−1291.

(21) Maldonado-Valderrama, J.; Rodríguez Patino, J. M. *Curr. Opin. Colloid Interface Sci.* **2010**, *5*, 271−282.
(22) Kovalchuk, V. I.; Kragel, J.; Makievski, A. V.; Ravera, F.; Liggieri, L.; Loglio, G.; Fainerman, V. B.; Miller, R. *J. Colloid Interface Sci.* **2004**, *280*, 498−505.
(23) Fainerman, V. B.; Leser, M. E.; Michel, M.; Lucassen-Reynders, E. H.; Miller, R. *J. Phys. Chem. B* **2005**, *109*, 9672−9677.
(24) Lee, L. T.; Mann, E. K.; Guiselin, O.; Langevin, D.; Farnoux, B.; Penfold, J. *Macromolecules* **1993**, *26*, 7046−7052.
(25) Muñoz, M. G.; Encinar, M.; Bonales, L. J.; Ortega, F.; Monroy, F.; Rubio, R. G. *J. Phys. Chem. B* **2005**, *109*, 4694−4699.
(26) Monroy, F.; Ortega, F.; Rubio, R. G. *Phys. Rev. E* **1998**, *58*, 7629−7941.
(27) Langevin, D. In *Light Scattering by Liquid Surfaces and Complementary Techniques*; Langevin, D., Ed.; Marcel Dekker: New York, 1992.
(28) Monroy, F.; Ortega, F.; Rubio, R. G.; Velarde, M. G. *Adv. Colloid Interface Sci.* **2007**, *134*−*35*, 175−189.
(29) Loglio, G.; Miller, R.; Stortini, A.; Tesei, U.; Innocenti, N. D.; Cini, R. *Colloids Surf. A* **1994**, *90*, 251−259.
(30) Liggieri, L.; Ferrari, M.; Mondelli, D.; Ravera, F. *Faraday Discuss.* **2005**, *129*, 125−40.
(31) Ravera, F.; Ferrari, M.; Liggieri, L. *Colloids Surf. A* **2006**, *282*, 210−216.
(32) Ritacco, H.; Feinerman, V. M.; Ortega, F.; Rubio, R. G.; Ivanova, N.; Starov, V. M. *Colloids Surf. A* **2010**, *365*, 204−209.
(33) Liggieri, L.; Santini, E.; Guzman, E.; Maestro, A.; Ravera, F. *Soft Matter* **2011**, *7*, 7699−7709.
(34) Maestro, A.; Ortega, F.; Rubio, R. G.; Rubio, M. A.; Krägel, J.; Miller, R. *J. Chem. Phys.* **2011**, *134*, 104704−104716.
(35) Rivillon, S.; Monroy, F.; Ortega, F.; Rubio, R. G. *Eur. Phys. J. E* **2002**, *9*, 375−385.
(36) Kotsmar, C.; Krägel, J.; Kovalchuk, V. I.; Aksenenko, E. V.; Fainerman, V. B.; Miller, R. *Langmuir* **2008**, *24*, 13977−13984.
(37) Gao, C.-S.; Yu, H.; Zografi, G. *J. Colloid Interface Sci.* **1994**, *162*, 214−221.
(38) Kovalchuk, V. I.; Krägel, J.; Makievski, A. V.; Ravera, F.; Liggieri, L.; Loglio, G.; Feinerman, V. B.; Miller, R. *J. Colloid Interface Sci.* **2004**, *280*, 498−505.
(39) Bain, C. D.; Claesson, P. M.; Langevin, D.; Meszaros, R.; Nylander, T.; Stubenrauch, C.; Titmuss, S.; von Klitzing, R. *Adv. Colloid Interface Sci.* **2010**, *155*, 32−49.
(40) Campbell, R. A.; Arteta, M. Y.; Angus-Smith, A.; Nylander, T.; Varga, I. *J. Phys. Chem. B* **2011**, *115*, 15202−15213.
(41) Alahverdjieva, V. S.; Grigoriev, D. O.; Ferri, J. K.; Fainerman, V. B.; Aksenenko, E. V.; Leser, M. E.; Michel, A.; Miller, R. *Colloids Surf. A* **2008**, *323*, 167−174.
(42) Mackie, A. R.; Gunning, A. P.; Ridout, M. J.; Wilde, P. J.; Patino, J. R. *Biomacromolecules* **2001**, *2*, 1001−1006.
(43) Gunning, A. P.; Kirby, A. R.; Mackie, A. R.; Kroon, P.; Williamson, G.; Morris, V. J. *J. Microsc.* **2004**, *216*, 52−56.
(44) Woodward, N. C.; Gunning, A. P.; Mackie, A. R.; Wilde, P. J.; Morris, V. J. *Langmuir* **2009**, *25*, 6739−6744.